Extremophiles (2017) 21:51–64
DOI 10.1007/s00792-016-0877-z

SPECIAL FEATURE: ORIGINAL PAPER

11th International Congress on Extremophiles

Differences in the phenotypic effects of mutations in homologous MrpA and MrpD subunits of the multi-subunit Mrp-type Na^+/H^+ antiporter

Masato Morino[1,4] · Shinichiro Ogoda[2] · Terry Ann Krulwich[1] · Masahiro Ito[2,3]

Received: 18 July 2016 / Accepted: 24 September 2016 / Published online: 5 October 2016

Abstract Mrp antiporters are the sole antiporters in the Cation/Proton Antiporter 3 family of transporter databases because of their unusual structural complexity, 6–7 hydrophobic proteins that function as a hetero-oligomeric complex. The two largest and homologous subunits, MrpA and MrpD, are essential for antiport activity and have direct roles in ion transport. They also show striking homology with proton-conducting, membrane-embedded Nuo subunits of respiratory chain complex I of bacteria, e.g., *Escherichia coli.* MrpA has the closest homology to the complex I NuoL subunit and MrpD has the closest homology to the complex I NuoM and N subunits. Here, introduction of mutations in MrpD, in residues that are also present in MrpA, led to defects in antiport function and/or complex formation. No significant phenotypes were detected in strains with mutations in corresponding residues of MrpA, but site-directed changes in the C-terminal region of MrpA had profound effects, showing that the MrpA C-terminal region has indispensable roles in antiport function. The results are consistent with a divergence in adaptations that support the roles of MrpA and MrpD in secondary antiport, as compared to later adaptations supporting homologs in primary proton pumping by the respiratory chain complex I.

Keywords Alkaliphiles · Cation/proton antiporter · Mrp · Complex I

Communicated by H. Atomi.

This article is part of a special feature based on the 11th International Congress on Extremophiles held in Kyoto, Japan, September 12–16, 2016.

Electronic supplementary material The online version of this article (doi:10.1007/s00792-016-0877-z) contains supplementary material, which is available to authorized users.

✉ Masahiro Ito
masahiro.ito@toyo.jp

Masato Morino
m.morino@sakaki.to

[1] Department of Pharmacological Sciences, Icahn School of Medicine at Mount Sinai, New York, NY 10029, USA

[2] Faculty of Life Sciences, Graduate School of Life Sciences, Toyo University, Oura-gun, Gunma 374-0193, Japan

[3] Bio-Nano Electronics Research Center, Toyo University, Kawagoe, Saitama 350-0815, Japan

[4] Present Address: 573-13 Kamitanui, Tarnaki-cho, Watarai-gun, Mie 519-0417, Japan

Introduction

Cation/proton antiporters have essential roles in cytoplasmic pH homeostasis and in adjusting cytoplasmic cation concentrations in both eukaryotic and prokaryotic cells (Padan et al. 2001; Brett et al. 2005; Orlowski and Grinstein 2007; Lee et al. 2013; Schuldiner 2014). Mrp-type antiporters, the only member of Cation/Proton antiporter-3 family of the Transporter Database, are widely distributed and have been found to play major roles in bacteria and archaea that need to be able to adapt to elevated salt and/or high pH environments (Ren et al. 2007; Saier et al. 2009). In addition, Mrp plays a role in the pathogenesis of some bacteria, e.g., *Pseudomonas aeruginosa* (Kosono et al. 2005). While most cation/proton antiporters are single gene products or their homo-dimers, Mrp antiporters consist of six or seven hydrophobic proteins, either an MrpA-B fusion and individual MrpC-G proteins, or seven individual MrpA-G proteins; the genes for the proteins are encoded in *mrp* operons (Swartz et al. 2005; Rimon et al. 2007). In

A

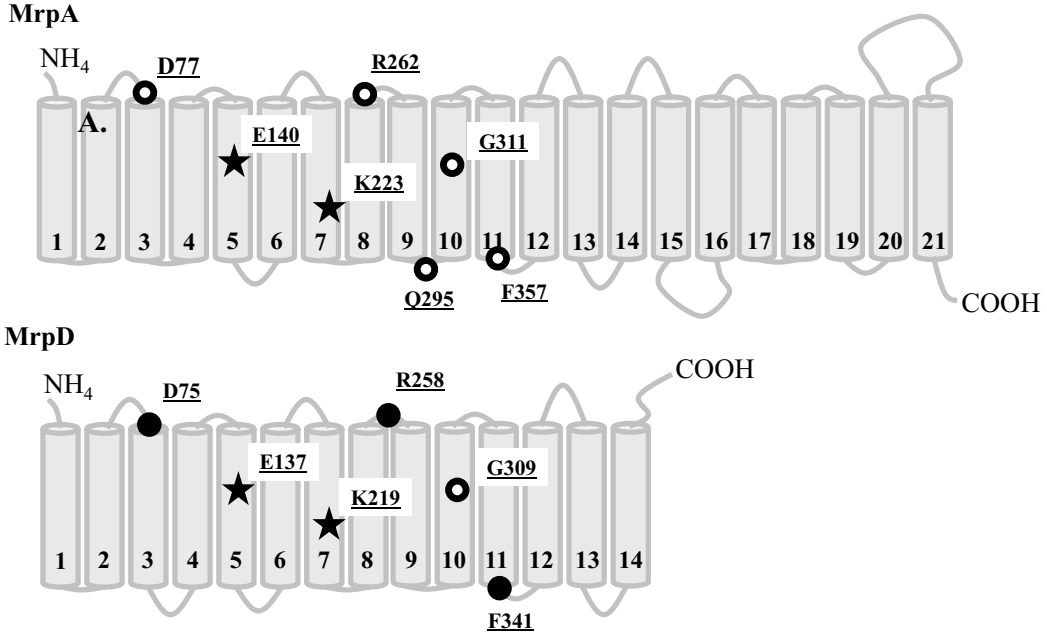

B

```
                                  TMS-3                                                  TMS-8
Bp_MrpA       67 SLGINFTVFVDGLSLLFALLITGIGTLVILYSIFYLSKK-(X134)-APTPVSAYLHSATMVKAGIYLV
Bh_MrpA       67 SLGINFTVYVDGLSLLFALLITGIGTLVALYSIYYLSKK-(X134)-APTPVSAYLHSATMVKAGLYLV
Bs_MrpA       67 SLGINFTVYIDGLGLLFALLITGIGSLVTLYSIFYLSKE-(X134)-APTPVSAYLHSATMVKAGIYVI
Sm_PhaA/B     94 ELGLNFTLRMDGFAWLFSALITAIGVLVALYARYYMAEE-(X133)-APTPVSAYLHSATMVKAGVFLL
Vc_MrpA/B     52 GLDLNLSFRLDGLSFLFASLITGIGALIQIYALAYMKEK-(X133)-APTPVSAYLHSATMVKAGIYLL
Bp_MrpD       65 QAPFGIVLVADLFATMMVILASIVGVVCLFFAFQTISSE-(X132)-GPPAAIAALFGGLLTKVGIYAI
Bh_MrpD       65 PAPFGIVLVADMFATMMIILSSIVGVACLFFAFQTISSE-(X132)-GPPAAIAALFGGLLTKVGIYAI
Bs_MrpD       65 KAPYGIVLAADQFASLLVLTTAIIGLLVGLYSFRSVGEK-(X132)-APPAAISALFGALLTKVGLYAI
Sm_PhaD       75 PAPFGIVLVLDRLSALMLCLTSGLALAAQAYSMARWHTA-(X132)-AATPPVAGVF-AVLTKVGIYVI
Vc_MrpD       66 PAPFGIVFVADLLSVGMVMVTAIIGLVSVIYAIADLSAK-(X131)-TLPSAIVALFAALLTKVGVYAL
Ec-NuoL       72 DFNIGFNLVLDGLSLTMLSVVTGVGFLIHMYASWYMRGE-(X135)-GPTPVSALIHAATMVTAGVYLI
Ec-NuoM       74 RFGISIHLAIDGLSLLMVVLTGLLGVLAVLCSWKEIEKY-(X138)-QAPTAGSVDLAGILLKTAAYGL
Ec-NuoN       60 AMDVTPLMRVDGFAMLYTGLVLLASLATCTFAYPWLEGY-(X135)-GAPAPVSTFLATASKIAIFGVV

                                  TMS-9                                  TMS-10
Bp_MrpA      261 ARLTPVFAGSAE------WFWLLTGFGVVTLLWGSTSAVRQKDLKGILAFSTVSQLGLIMTLLGLGSAA
Bh_MrpA      261 ARLTPVFGGTPE------WFWLLAGFGIITLCWGSISAVRQKDLKSILAFSTISQLGLIMCLFGLGSAT
Bs_MrpA      261 ARFSPIFAFSAQ------WFWIVSLVGLFTMVWGSFHAVKQTDLKSILAFSTVSQLGMIISMLGVSAAA
Sm_PhaA/B    287 VRFWPVMAGTEA------WFWIVGLAGLTTLLLGAYFAIFQQDLKGLLAYSTISHLGLITVLLSLGSP-
Vc_MrpA/B    245 ARLSPIYASSDF------WFYCLTIVGAVTALWCALLAFKQTDLKLMLAYSTNVALGKLTLLLGLGTE-
Bp_MrpD      257 MRTFTLIFNHDP----GFTHTLILILAGLTMFFGVLGAVSQFDFKRILSYHIISQVGYMVMGLGIYTQ-
Bh_MrpD      257 IRTFTLIFNHDP----SFTHTIILALAGFTMFFGVLGAVSQFDFKRILSYHIISQVGYMVMGLGIFTP-
Bs_MrpD      257 TRVFTLIFIHDT----AFTHQLMIWLAALTVIFGVIGSLAYSNVMKIVIYNIITAVGVILFGVAVHTP-
Sm_PhaD      266 IRLHLLVFGTAAGASSGFGQEWLVTGGMLTIAFGGIGVLASQAMGRLAGYSVLVSSGTLLAAVGLGHD-
Vc_MrpD      257 LRVFTLVFPLDG----SGWQPVLLGIAALTMLTGVLGAASQYDIKKILSFHIISQIGYMIMGLAIYTP-
Ec-NuoL      267 ARTHGLFLMTPE------VLHLVGIVGAVTLLLAGFAALVQTDIKRVLAYSTMSQIGYMFLALGVQAW-
Ec-NuoM      272 LRFSLPLFPNAS----AEFAPIAMWLGVIGIFYGAWMAFAQTDIKRLIAYTSVSHMGFVLIAIYTGSQ-
Ec-NuoN      255 MRLFLYAPVGDS----EAIRVVLAIIAFASIIFGNLMALSQTNIKRLLGYSSISHLGYLLVALIALQTG

                                  TMS-11
Bp_MrpA      324 IYFG-ESVDPAFYSFAIMAAIFHLINHATFKGSLFMTAGIIDHETGT
Bh_MrpA      324 LHFDPTDSMIKFYATATLAAVFHLINHATFKGSLFMTVGIIDHETGT
Bs_MrpA      324 LHYG----HTEYYTVAAMAAIFHLINHATFKGSLFMAVGIIDHETGT
Sm_PhaA/B    349 --------------LAAVAAVFHIVNHATFKASLFMAAGIIDHESGT
Vc_MrpA/B    307 --------------VALTAAVLFIFAHSFYKAALFMVVGNIDKATGT
Bp_MrpD      321 --------------LAIAGAIYYIAHHIIVKAALFLFAGATQRITGT
Bh_MrpD      321 --------------LALAGAIYYIAHHIIVKAALFLFAGATEKITGT
Bs_MrpD      321 --------------ASIQGAIYYLIHDMLIKGALFMLAGTLIALTGT
Sm_PhaD      334 --------------GMLAGALFYLVSSTLTIGAFFLLIELVERGRDA
Vc_MrpD      321 --------------LAITGAIFYVIHHILVKGNLFLIGGLIGRKYGT
Ec-NuoL      329 ------------------DAAIFHLMTHAFFKALLFLASGSVILACHH
Ec-NuoM      336 --------------LAYQGAVIQMIAHGLSAAGLFILCGQLYERIHT
Ec-NuoN      320 --------------EMSMEAVGVYLAGYLFSSLGAFGVVSLMSSPYRG
```

◂**Fig. 1** Positions of essential charged amino acid residues and mutated residues in MrpA and MrpD. **a** The residues in which a mutation reduced the antiport activity to 75 % or less of the wild type activity are indicated by *filled circles*. The *open circles* represent residues in which mutation exhibited wild type activity. The *filled stars* represent residues in which a mutation led to loss of both Na^+/H^+ antiporter activity and Na^+ tolerance in previous work (20). **b** Multi-alignment analyses around residues in which we introduced mutations in this study. The target residues are indicated by *bold*. The *gray highlighted* residues represent the TMSs; for MrpA and MrpD, the TMSs except for the 8th TMS were predicted by all three programs. The 8th TMS was predicted by only two programs, HMMTOP and TMHMM. Details are described in Experimental Procedures. For NuoLMN subunits, the proposed structures reflect data from crystal structures (Baradaran et al. 2013)

extremophilic alkaliphiles that grow under non-fermentative conditions, the Mrp antiporter has an essential role in cytoplasmic pH homeostasis in their upper pH ranges, which in alkaliphilic *Bacillus pseudofirmus* OF4 is as high as pH 11.2 (Sturr et al. 1994).

In the antiport reaction of the Mrp antiporter of *B. pseudofirmus* OF4, Mrp-dependent efflux of sodium ions is coupled to electrogenic uptake of a greater number of protons, which are imported against their chemical gradient. This electrogenic exchange is energized by the transmembrane electrical potential of the proton motive force that is generated by respiration (Krulwich et al. 2011). Mrp-dependent sodium efflux also maintains an inwardly directed sodium gradient that energizes motility and a large number of cation/solute symporters of alkaliphilic *Bacillus* spp. (Padan et al. 2005; Krulwich and Ito 2013). There is not yet structural information for a secondary cation/proton antiporter of the Mrp-type that could enable simulations such as those of "water wires" that are involved in rapid unidirectional proton transfers in a complex I membrane domain that has significant resemblance to segments of Mrp (Kaila et al. 2014). Among the 7 Mrp subunits of *B. pseudofirmus* OF4, MrpA and MrpD show similarities to each other as well as to subunits of respiratory chain complex I (NADH: ubiquinone oxidoreductase), as was noted when the partial sequence of the Mrp of an alkaliphilic *Bacillus* was first reported by Hamamoto et al. (Hamamoto et al. 1994). Deletions of *mrp* in *B. pseudofirmus* OF4 have thus far been lethal, whereas a *mrp* null mutant and in-frame deletion mutants of each *mrp* gene of *Bacillus subtilis* are viable (Ito et al. 2000; Padan et al. 2005). The NuoL, NuoM and NuoN subunits of the complex I of *Escherichia coli* are referred to as "antiporter"-like subunits, along with the smaller NuoK, which most closely resembles MrpC (Mathiesen and Hägerhäll 2003). These subunits have striking regions of homology with Mrp antiporter subunits and are proposed to dominate the proton-conducting membrane domain of complex I (Efremov and Sazanov 2011). In complex I, these membrane domains contain the paths taken by protons that are pumped out of the membrane domains using the energy obtained by coupling of this domain to a hydrophilic electron transport domain, the 'peripheral arm' (Efremov and Sazanov 2011; Steimle et al. 2012; Baradaran et al. 2013). By contrast, the transmembrane proton motive force provides the energy for the electrogenic cation/proton exchange catalyzed by Mrp antiporters, which lack a peripheral arm (Swartz et al. 2005; Morino et al. 2008). In this study, the effects of mutations in MrpA and MrpD were examined in the context of evidence that MrpA catalyzes Na^+ efflux, while MrpD catalyzes uptake of a greater number of H^+; in *B. subtilis*, these two Mrp subunits can be replaced partially by NuoL and NuoN, respectively (Moparthi et al. 2014). Further, Mrp antiporter subunits are proposed to be contributors to the evolution of respiratory chain complex I as well as related hydrogenases (Moparthi and Hägerhäll 2011a, b).

Mutagenesis analyses have shown that MrpA and MrpD residues that are important for ion exchange are found in homologs positions in their Nuo homologs, i.e., MrpA-E140, MrpA-K223, MrpD-E137 and MrpD-K219 (Fig. 1a) (Torres-Bacete et al. 2007; Morino et al. 2010; Nakamaru-Ogiso et al. 2010; Sato et al. 2013). Crystal structures of *E. coli* complex I showed that the "antiporter"-like subunits have a common conformational feature, an anti-parallel repeat structure composed of 14 transmembrane segments (TMS) (Amarneh and Vik 2010; Efremov and Sazanov 2011; Baradaran et al. 2013; Virzintiene et al. 2013). The region from the N-terminus to the putative 14th transmembrane helices of Nuo is well conserved in both MrpA and MrpD. MrpA has a unique additional region in the C-terminus, the A-CT (C-terminal extension of the MrpA) region. This region was referred to by Virzintiene et al. (2013) as "the evolutionary progenitor of the long horizontal helix in complex I". The NuoJ subunit of the NuoAJK domain, that is near the bend toward the peripheral arm, originates in A-CT (Morino et al. 2010; Moparthi and Hägerhäll 2011b).

In this study, we introduced site-directed mutations into amino acid residues conserved across MrpA, MrpD, NuoL, NuoM and NuoN to probe functional differences between MrpA and MrpD using a comparison framework that includes the Nuo homologs. Effects of mutations of the A-CT region of MrpA were also examined to clarify their contributions to antiport activity and Mrp complex assembly.

Materials and methods

Bacterial strains, culture conditions and plasmids

The bacterial strains and plasmids used in this study are listed in Table 1 with their properties and sources. *E. coli*

Table 1 Bacterial strains and plasmids used in this study

Strain or plasmid	Genotype	References or source
Escherichia coli		
DH5α MCR	F$^-$ *mcrA*Δ*1* (*mrr-hsd RMS-mcrBC*) 80*dlacZ*Δ(*lacZYAargF*)*U169 deoR recA1 endA1 supE44* λ*thi-1 gyr-496 relA1*	Stratagene
KNabc	TG1 (Δ*nhaA* Δ*nhaB* Δ*chaA*)	(Nozaki et al. 1998)
Plasmids		
pGEM7zf (+)	Cloning vector, Amp^r	Promega
pGEMmrpTFCHS7	pGEM7zf(+) + *mrp* operon from *B. pseudofirmus* OF4 (MrpA-T7, MrpB-FLAG, MrpC-*c* myc, MrpD-His and MrpG-S tag)	(Morino et al. 2008)
pGEMmrpTFCHS7 MrpA-D77A	pGEMmrpTFCHS7 + MrpA-D77A mutation	This study
pGEMmrpTFCHS7 MrpA-D77E	pGEMmrpTFCHS7 + MrpA-D77E mutation	This study
pGEMmrpTFCHS7 MrpA-R262A	pGEMmrpTFCHS7 + MrpA-R262A mutation	This study
pGEMmrpTFCHS7 MrpA-Q295A	pGEMmrpTFCHS7 + MrpA-Q295A mutation	This study
pGEMmrpTFCHS7 MrpA-G311A	pGEMmrpTFCHS7 + MrpA-G311A mutation	This study
pGEMmrpTFCHS7 MrpA-F357A	pGEMmrpTFCHS7 + MrpA-F357A mutation	This study
pGEMmrpTFCHS7 MrpA-F671A	pGEMmrpTFCHS7 + MrpA-F671A mutation	This study
pGEMmrpTFCHS7 MrpA-P677G	pGEMmrpTFCHS7 + MrpA-P677G mutation	This study
pGEMmrpTFCHS7 MrpA-T683A	pGEMmrpTFCHS7 + MrpA-T683A mutation	This study
pGEMmrpTFCHS7 MrpA-E687A	pGEMmrpTFCHS7 + MrpA-E687A mutation	This study
pGEMmrpTFCHS7 MrpA-P702G	pGEMmrpTFCHS7 + MrpA-P702G mutation	This study
pGEMmrpTFCHS7 MrpA-R773A	pGEMmrpTFCHS7 + MrpA-R773A mutation	This study
pGEMmrpTFCHS7 MrpA-E780A	pGEMmrpTFCHS7 + MrpA-E780A mutation	This study
pGEMmrpTFCHS7 MrpD-D75A	pGEMmrpTFCHS7 + MrpD-D75A mutation	This study
pGEMmrpTFCHS7 MrpD-D75E	pGEMmrpTFCHS7 + MrpD-D75E mutation	This study
pGEMmrpTFCHS7 MrpD-R258A	pGEMmrpTFCHS7 + MrpD-R258A mutation	This study
pGEMmrpTFCHS7 MrpD-G309A	pGEMmrpTFCHS7 + MrpD-G309A mutation	This study
pGEMmrpTFCHS7 MrpD-F341A	pGEMmrpTFCHS7 + MrpD-F341A mutation	This study

strains, DH5α MCR (GibcoBRL) (wild type) and KNabc (antiporter-deficient) strains (Nozaki et al. 1998) were, respectively, used in this study for routine genetic manipulations or assay of mutated Mrp antiporters. The *E. coli* KNabc transformants were grown in LBK medium (1 % tryptone, 0.5 % yeast extract and 83 mM KCl pH 7.5). For the preparation of membrane vesicles, the transformants were grown at 37 °C for 16 h in LBK-Na medium (1 % tryptone, 0.5 % yeast extract, 83 mM KCl and 50 mM NaCl pH 7.5). Ampicillin and kanamycin were added to a final concentration of 0.1 and 0.025 mg/ml.

Construction of site-directed mutants and A-CT deletion mutants

Amino acid-substituted mutation plasmids were made using pGEMmrp TFCHS7 (Morino et al. 2008), which encodes the *B. pseudofirmus* OF4 *mrpABCDEFG* operon with a T7 tag, FLAG (DDDDK) tag, *c*-myc tag, His_7 tag and S tag sequence fused to the *mrpA*, *mrpB*, *mrpC*, *mrpD* and *mrpG* genes and containing its putative promotor region, respectively. MrpE and MrpF proteins were detected by anti-MrpE antibody and anti-MrpF antibody, respectively. Goat-anti-Rabbit HRP (Bio-Rad) was also used as the second antibody for detection of anti-MrpE and anti-MrpF antibodies. For introduction of site-directed mutations in vitro, the Gene Tailor™ site-directed mutagenesis system (Invitrogen) was used, following the procedure previously reported (Morino et al. 2010). To identify the conserved amino acid residues, ClustalW2 (http://www.ebi.ac.uk/Tools/msa/clustalw2/) was used. Amino acid sequence sources are Bp-Mrp from *B. pseudofirmus* OF4, Bh-Mrp from *Bacillus halodurans* C-125, Bs-Mrp from *B. subtilis* 168, Sm-Pha from *Sinorhizobium meliloti* (in which Mrp

is named Pha) and Vc-Mrp from *Vibrio cholerae*. Secondary structure predictions for MrpA and MrpD were carried out previously using three programs: ConPred II (http://bioinfo.si.hirosaki-u.ac.jp/~ConPred2/), HMMTOP (http://www.enzim.hu/hmmtop/), and TMHMM (http://www.cbs.dtu.dk/ services/TMHMM/). All primer sequences are provided in Table S1.

Membrane preparations from *E. coli* transformants

The preparation of everted membrane vesicles from *E. coli* KNabc transformants was accomplished using a standard procedure (Morino et al. 2008). Briefly, cells were grown, harvested and then washed by with TCDG buffer (10 mM Tris–HCl pH 8.0, 5 mM $MgCl_2$ and 10 % glycerol, 140 mM choline Cl and 1 mM D-dithiothreitol). The cell suspension was passed through a French press (10,000 psi). After centrifugations at 7000 and 26,000*g*, each for 10 min, the membrane fraction was collected by ultracentrifugation at 180,000*g* for 90 min and then suspended in fresh TCDG buffer. The membrane fraction was stored at −80 °C. Protein content was determined by the Lowry method using lysozyme as a standard (Lowry et al. 1951).

Na^+/H^+ antiport activity in the everted membrane vesicles

Escherichia coli KNabc membrane vesicles (66 μg protein) were diluted into 2 ml of assay buffer (10 mM bis–tris phosphonate (BTP)-Cl, 5 mM $MgCl_2$, 100 mM cholineCl) supplemented with 1 μM acridine orange. The assay was initiated by adding succinate to a final concentration of 2.5 mM. After steady-state fluorescence quenching was reached, NaCl was added to a final concentration of 1 mM. Finally, 1 mM NH_4Cl was added to the assay buffer to abolish any ΔpH and establish a baseline. Using the baseline, % dequenching, a decrease in the succinate-dependent ΔpH due to Na^+ addition, was calculated by tracing the fluorescent changes. In this study, the Na^+/H^+ antiport activities of each mutant were represented by normalizing % dequenching to that of wild type. The % dequenching from empty vector control vesicles was subtracted from every value from both wild type (pGEMmrpTFCHS7) and mutant vesicles, i.e., the normalized Na^+/H^+ antiport activity of wild type and empty vector control vesicles, respectively, is 100 and 0. The concentration of Na^+ yielding the half-maximal dequenching has been validated as a good estimate of the apparent K_m of Na^+/H^+ antiporters (Swartz et al. 2007).

Western blots and Blue Native-PAGE analyses

Western blots and Blue Native Polyacrylamide Gel Electrophoresis (BN-PAGE) were performed as described previously (Morino et al. 2008). In western blots, each Mrp subunit was detected using polyclonal antibodies commercially available; anti-T7 tag, FLAG tag, *c*-myc tag, S tag and His_6 tag antibodies conjugated with horse radish peroxidase (HRP) were purchased from Abcam. MrpE and MrpF proteins were detected using antibodies specific for their peptide sequences.

Results

Multi-alignment analysis of MrpA and MrpD homologs

In this study, we introduced alanine substitutions into positions of the following eight residues: MrpA-D77, MrpA-R262, MrpA-G311, MrpA-F357, MrpD-D75, MrpD-R258, MrpD-G309, and MrpD-F341 (Fig. 1). These are conserved in all five homologs of Mrp and Nuo, MrpA, MrpD, NuoL, NuoM and NuoN. The additional replacements were glutamic acid for MrpA-D77 and MrpD-D75 to observe the side-chain replacement effect. A MrpA-Q295A construct was also included in the mutant panel because this residue is highly conserved in MrpA and NuoLMN subunits.

Differences between the phenotypes of antiporter with MrpA or MrpD mutations

The impact of the mutations on the activity, expression and complex formation was characterized by expressing each of the mutant antiporter forms from plasmids in antiporter-deficient *E. coli* KNabc. The phenotypes of the mutants are summarized in Table 2. The functional effects were elucidated by growth tests in *E. coli* KNabc transformants and fluorescence-based Na^+/H^+ antiport assays in everted membrane vesicles. While *E. coli* KNabc transformed with pGEM7zf (+), the empty vector, showed no growth in LBK medium containing 0.2 M NaCl, the transformants with the tagged wild type antiporter, pGEMmrpTFCHS7, grew in LBK medium with as much as 0.5 M NaCl (Fig. 2). In the antiport assays shown in Fig. 3, all the antiporters with MrpA mutant forms exhibited similar Na^+/H^+ antiport activity to wild type (MrpTFCHS7). By contrast, two of the antiporters with MrpD mutants, MrpD-D75A and MrpD-R258A, showed significantly reduced activity and smaller, but detectable, defects were observed in activity of antiporters containing MrpD-D75E or MrpD-F341A mutations. Transformants of *E. coli* KNabc expressing an MrpD-D75A mutant failed to grow in LBK medium at pH 7.5 even without added NaCl (Fig. 2d). Since such inhibition was not observed at pH 7.0, the MrpD-D75A transformant was cultured at pH 7.0 for later assays. In the membrane vesicles from transformants expressing MrpD-D75A, the antiport activity was only 10 % of wild type (Table 2;

Table 2 Summary of the effects of single mutations in MrpA and MrpD and of truncations in MrpA

E. coli KNabc transformants			Support of *E. coli* KNabc growth		Na^+/H^+ Antiport						Expression							Complex		
			Growth in LBK medium plus		% of wt Na^+/H^+ antiport activity[a]			Apparent K_m values for Na^+ (mM)			Expression levels calculated from western blots[c]							Complex formation[d]		
			200 mM NaCl	500 mM NaCl	pH 8.0	pH 8.5	pH 9.0	pH 8.0	pH 8.5	pH 9.0	MrpA	MrpB	MrpC	MrpD	MrpE	MrpF	MrpG	Dimeric Full complex	Monomeric Full complex	MrpA-D Subcomplex
pGEM7zf(+) (negative control)			–	–	0	0	0	nd	nd	nd	0	0	0	0	0	0	0	–	–	–
pGEMmrpTFCHS7 (tagged wt *mrp*)			+	+	100	100	100	0.165	0.096	0.092	1	1	1	1	1	1	1	+	+	+
MrpAD corresponding mutations	MrpA	D77A	+	+	80.4 ±1.5	99.0 ±6.8	95.7 ±4.6	nd	nd	nd	0.98	1.05	0.98	0.91	0.98	1.18	0.82	+	+	+
		D77E	+	+	87.1 ±3.7	83.6 ±8.6	94.6 ±0.8	nd	nd	nd	1.1	1.02	0.99	0.82	1.11	1.25	0.77	+	+	+
		R262A	+	+	93.6 ±7.1	96.4 ±3.1	100.4 ±2.0	nd	nd	nd	1.02	1.04	1.07	0.87	1.22	1	0.98	+	+	+
		Q295A	+	+	100.2 ±0.0	90.9 ±8.1	92.2 ±3.6	nd	nd	nd	0.75	1.05	1.06	0.74	0.51	1	1	+	+	+
		G311A	+	+	84.4 ±2.7	96.7 ±4.8	94.7 ±3.8	nd	nd	nd	0.95	1.06	1.02	0.83	1.2	1.24	0.87	+	+	+
		F357A	+	+	86.5 ±8.0	93.4 ±9.4	77.0 ±1.0	nd	nd	nd	0.97	1.02	1.01	0.8	1.02	1.01	0.96	+	+	+
	MrpD	D75A[b]	–	–	3.8 ±1.2	7.1 ±0.6	9.9 ±2.7	nd	nd	nd	0.18	0.04	0.49	0.07	0.06	0.08	0.13	–	–	–
		D75E	+	+	71.4 ±3.3	68.5 ±2.5	63.5 ±9.1	0.095	0.056	0.059	0.66	0.68	0.92	0.57	0.87	0.7	0.81	+	+	+
		R258A	–	–	21.3 ±1.2	29.6 ±3.4	32.8 ±6.3	0.095	0.064	0.067	0.06	0.1	0.49	0.1	0.13	0.05	0.01	–	–	–
		G309A	+	+	84.0 ±7.5	87.7 ±0.4	76.9 ±1.4	nd	nd	nd	0.57	0.89	0.89	0.71	1.19	1.11	0.96	+	+	+
		F341A	+	–	56.4 ±3.5	64.1 ±0.5	65.5 ±7.8	0.45	0.463	0.366	0.57	0.53	0.86	0.59	0.51	0.57	0.77	+	+	+
A-CT (C-terminal extension of the MrpA) region mutations		F671A	+	+	79.0 ±1.1	78.8 ±1.0	89.0 ±7.8	nd	nd	nd	1.15	0.98	1.04	0.99	1.24	1.15	0.97	+	+	+
		P677G	+	+	81.3 ±5.2	83.7 ±2.1	82.2 ±4.4	nd	nd	nd	1.08	0.92	0.74	1.05	0.91	1.25	0.92	+	–	+
		T683A	+	+	82.6 ±8.0	86.8 ±7.3	85.6 ±1.5	nd	nd	nd	1.04	0.94	0.88	0.92	1.09	0.98	0.7	+	+	+
		E687A	–	–	0.1 ±0.1	0.7 ±0.7	1.3 ±0.6	nd	nd	nd	0.8	0.66	0.82	0.57	0.54	0.77	0.48	+	+	+
		P702G	+	+	33.1 ±5.2	33.8 ±5.6	31.1 ±5.2	0.401	0.326	0.321	0.8	0.55	0.49	0.88	0.45	0.64	0.53	+	+	+
		R773A	–	–	0.0 ±0.0	1.0 ±1.0	0.7 ±0.7	nd	nd	nd	0.3	0.18	0.52	0.78	0.21	0.27	0.18	+	+	+
		E780A	–	–	0.3 ±0.8	0.0 ±0.0	1.2 ±1.5	nd	nd	nd	0.68	0.74	0.6	0.84	0.46	0.5	0.52	+	+	+

nd = not determined (see text for criteria for which assays where omitted)

[a] % Na^+/H^+ antiport values are normalized to that of the tagged wild type MrpTFCHS7 activity. Details of the methods for preparation and assays of membrane vesicles are described under Experimental Procedures. The values presented for the percent dequenching are average values from duplicate assays from three independent experiments. These values for percent dequenching are shown with the standard deviation of the values

[b] The *E. coli* KNabc transformed with MrpD-D75A was grown in LBK medium at pH 7.0 for membrane vesicle preparations

[c] A quantitative imaging system, Pluor-S MAX (Bio-Rad), was used for detection and analysis of a chemiluminescence image. Values in table indicate the ratio of expression level of each Mrp protein as compared with that of MrpTHCHS7

[d] The clear presence of multiple Mrp proteins at hetero-oligomer positions is scored as a " + " in the Mrp A-G dimer or monomer column or MrpA-D sub-complex column even if one or more Mrp proteins is not well resolved as SDS-PAGE. Dark gray highlights indicate mutant phenotypes that differ markedly from the wild type transformant, e.g., inability to grow in the presence of 200 or 500 mM added NaCl, major defects in Na^+/H^+ antiporter activity, decreases in the membrane levels of Mrp proteins of ≥60 %, or the absence of one or more Mrp complexes in BN-PAGE analyses. Mutants in which the Na^+/H^+ antiporter activity is at least 35 % lower than wild type are highlighted in light blue. Mutants in which the apparent K_m is at least 2.4 higher than that of wild type Mrp are highlighted in dark blue. Mutants in which the expression level of Mrp proteins in membrane vesicles is ≤30 % of the positive control are highlighted in yellow

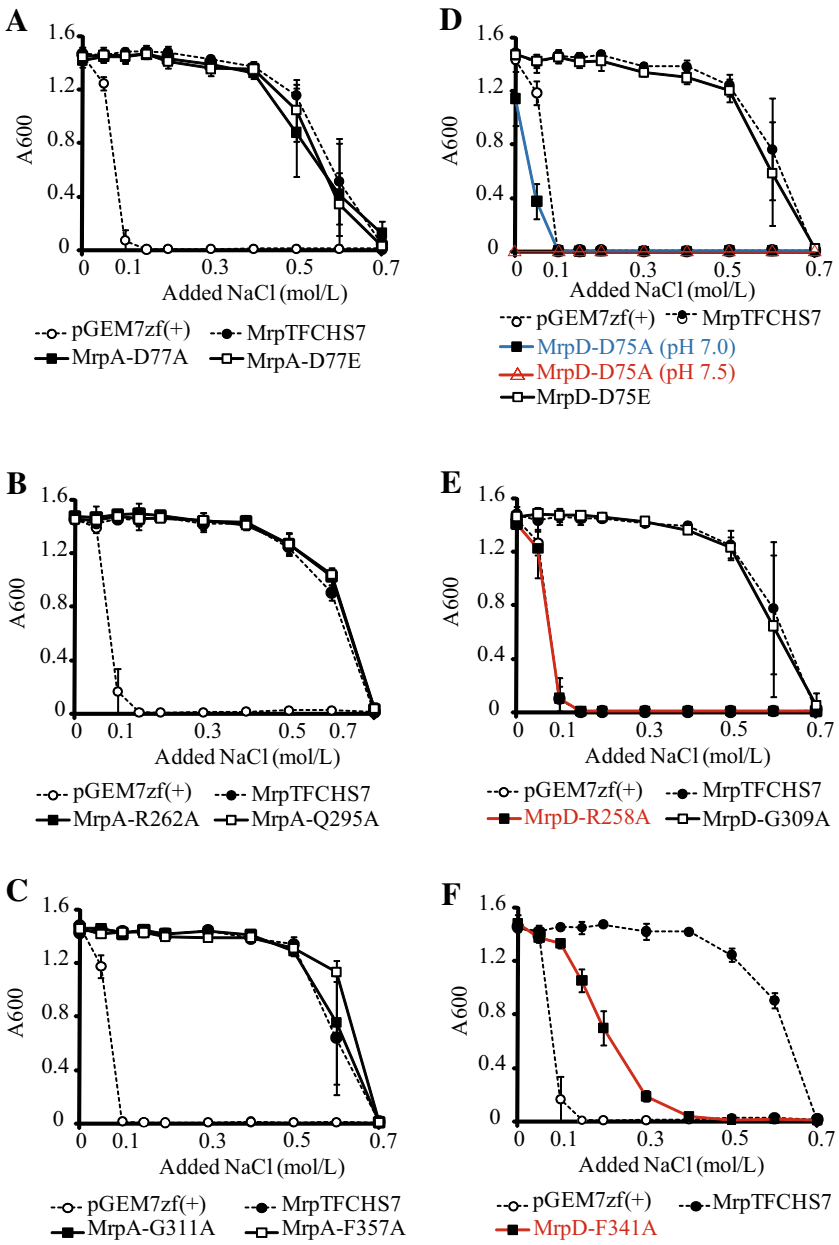

Fig. 2 Effect of mutations on the capacity of Mrp antiporter to complement the sodium sensitivity of *E. coli* KNabc. *E. coli* KNabc transformants were grown at 37 °C for 16 h in LBK medium, at pH 7.5, containing added NaCl at the indicated concentrations. Growth of MrpD-D75A transformant was no growth at pH 7.5. Therefore, this transformant was also grown at pH 7.0. The A_{600} of the cultures was then measured. The *error bars* indicate standard deviations for the results from duplicate cultures in three independent experiments. *Red lines* in each graph indicate mutant phenotypes that differ markedly from the wild type transformant

Fig. 3). By contrast, the MrpD-D75E residue retained more substantial antiport activity, about 68 % of wild type and the apparent K_M value was reduced 1.6-fold compared to wild type, suggesting that an acidic amino acid residue at the position of MrpD-D75 is critical for optimum enzymatic activity. MrpD-R258A and MrpD-F341A mutations also led to decreases in antiport activity, to about 28 and 62 % of wild type, respectively (Table 2; Fig. 3). The MrpD-R258 mutant retained a wild K_M value while the K_M value of the MrpD-F341A mutant was about 4 times higher than the wild type at pH 9.0, a typical growth pH for the alkaliphile (Table 2).

In a previous study, the *B. pseudofirmus* OF4 Mrp antiporter was shown to form three complexes, monomeric and dimeric full-Mrp complexes that contain all seven Mrp subunits and an inactive MrpABCD sub-complex (Morino et al. 2008). Here, we used BN-PAGE analyses to probe any changes in the distribution of Mrp complexes caused by the site-specific mutations (Fig. 4a–g). In the membrane vesicle assays of antiporters with MrpD-D75A or MrpD-R258A mutations, no Mrp complexes were detectable. The levels of Mrp subunits were also decreased, relative to a tagged wild type, in the membranes from the MrpD-D75A and MrpD-R258A mutants (Fig. 4h; Table 2). For the other mutants, all complexes were observed.

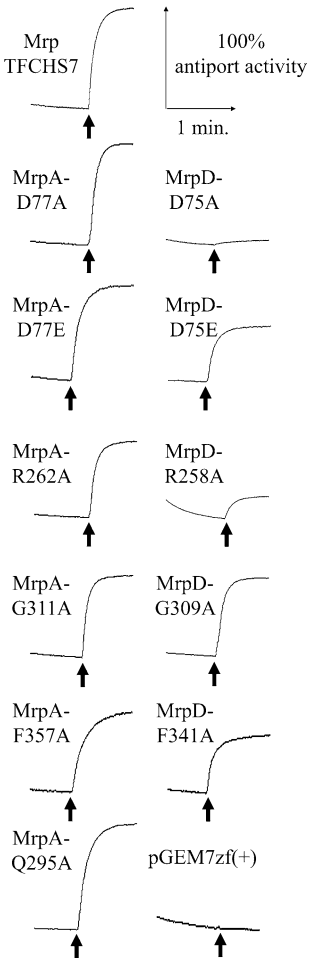

Fig. 3 Fluorescence-based assays of Na^+/H^+ antiport activity of MrpA and MrpD mutants. The assay was initiated by addition of succinate to 1 mM. After a succinate-dependent ΔpH formed, inside acid relative to outside, across the everted membrane vesicles, NaCl was added to 1 mM. The time point for the NaCl addition is indicated by an upward arrow. Each *figure* shows a trace of fluorescence change following NaCl addition. This dequenching, calculated as % of wild type, is used as the measure of antiport activity. Typical averages of % dequenching by the wild type Mrp antiporter are: at pH 8.0: 54.7 ± 8.3; at pH 8.5: 55.6 ± 8.9; and at pH 9.0: 53.1 ± 9.3

The A-CT region is involved in both antiport activity and complex formation

To clarify the roles of the A-CT region of MrpA, we constructed a set of site-directed alanine substitution mutants at conserved residues, except for MrpA-P677 and MrpA-P702, which were replaced by glycine, whose flexibility is closer than that of alanine to proline (Fig. 5). Two glutamate residues, MrpA-E687 and MrpA-E780, located in a putative transmembrane helix had already been reported to be essential for the antiport activity in Mrp from *Bacillus subtilis* (Kajiyama et al. 2009). Here, the corresponding acidic residues in *B. pseudofirmus* OF4 Mrp were mutated, as were several adjacent residues. The transformants of *E. coli* KNabc expressing MrpA-E687A, MrpA-R773A and MrpA-E780A mutants exhibited a loss of Na^+ tolerance to growth in LBK medium (Fig. 6). The Na^+/H^+ antiport assays (Fig. 7) showed that the MrpA-E687A, -R773A and -E780A mutants of the alkaliphile Mrp displayed no antiport activity. Additionally, the MrpA-P702G mutation resulted in a decrease in antiport activity to about 33 % of wild type (Table 2) while the K_M value was about 3.5-fold higher than the wild type value at pH 9.0. For MrpA-F671A, -P677G and T683A mutants, 79–89 % of antiport activity, compared to wild type, was observed in the antiport assays. In the BN-PAGE analyses (Fig. 8a–g), no monomeric full-Mrp complex was detected in the MrpA-P677G mutant, while the dimeric full-Mrp complex and the MrpABCD sub-complex were observed. All three types of Mrp complexes were detected in the other mutants. The levels of Mrp subunits of MrpA-R773A mutant were decreased relative to a tagged wild type (Fig. 8h; Table 2). For other mutants, all complexes were observed.

Discussion

In this study, a panel of mutations was made in MrpA and MrpD, the two largest subunits of the 7-subunit Na^+/H^+ Mrp antiporter of alkaliphilic *Bacillus pseudofirmus* OF4 (Sturr et al. 1994; Padan et al. 2005; Krulwich et al. 2011; Krulwich and Ito 2013; Kaila et al. 2014). The significant homology between MrpA and MrpD and one or more membrane subunits of respiratory complex I creates the opportunity to see whether MrpA and MrpD differ with respect to the importance of their regions of homology with their most closely related complex I subunit(s). For example, if "antiporter-like" NuoL has substantially or entirely replaced the sodium-related features of its MrpA progenitor with proton-pumping elements, then deleting those proton-pumping elements would not be expected to have an effect on MrpA (Moparthi et al. 2011). By contrast, both MrpD and its homologous "antiporter-like" NuoM and N translocate protons. MrpD moves protons inward as part of the electrogenic exchange with the sodium that is effluxed by MrpA. On the other hand, NuoM and N release protons using energy made available through its interactions as part of full primary pumping complex I. Although the energization mode is different, use by MrpD of the domain resembling that of NuoM and N is consistent with their roles in translocating protons. By contrast, MrpA is responsible for the sodium-translocation function of the antiporter while the NuoL subunit of the complex I membrane subunits is significantly, if not entirely, adapted to translocate protons. Indeed, the marked difference in the impact of mutations in parallel locations of MrpA and MrpD is one of

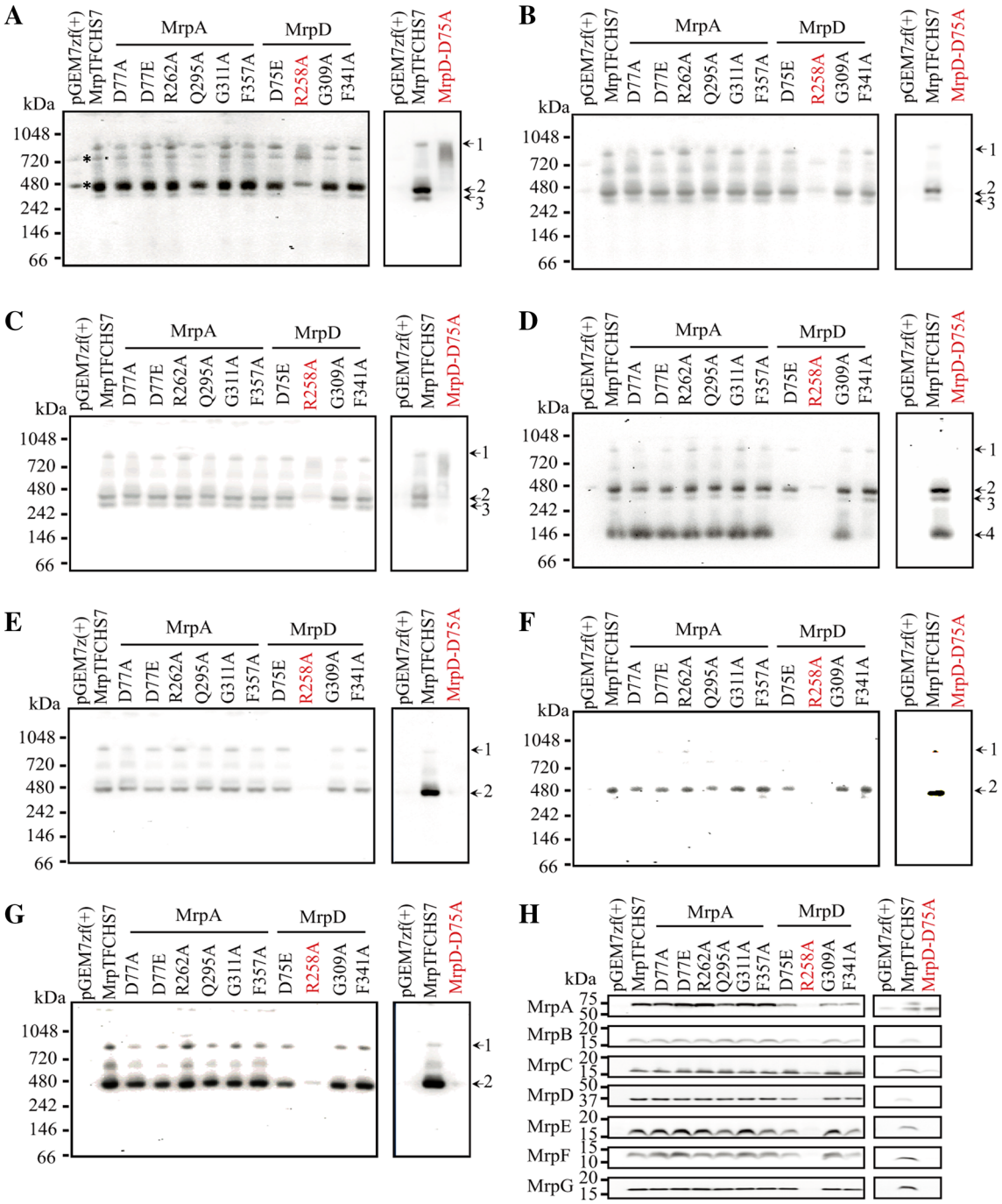

Fig. 4 BN-PAGE and SDS-PAGE analyses and western blot analysis of MrpA and MrpD mutants. For BN-PAGE, the proteins (30 μg) extracted from the everted membrane fraction were loaded on a precast gel (4–16 % acrylamide, invitrogen). For BN-PAGE, MrpA (**a**), MrpB (**b**), MrpC (**c**), MrpD (**d**), MrpE (**e**), MrpF (**f**) and MrpG (**g**) proteins were detected by western blot using anti-T7 tag antibody, anti-FLAG (DDDDK) tag antibody, anti-*c*-myc tag antibody, anti-penta His tag antibody, anti-MrpE peptide antibody, anti-MrpF peptide antibody or anti-S-tag antibody, respectively. For comparison of expression levels of Mrp subunits in the mutants, thirty micrograms of membrane vesicle protein was applied to SDS-PAGE gels following western blot (H). The *arrow* plus *number* 1, 2, 3 and 4 on the right of each BN-PAGE panel indicates the position of the MrpABCDEFG dimmer, the MrpABCDEFG monomer, the stable MrpABCD sub-complex, and the MrpD dimer (MrpDD), respectively. The *asterisks* in panel (**a**) indicate a non-specific band. Mutants shown in *red* indicate a decrease in the membrane levels of Mrp protein of ≥60 %,or the absence of one or more Mrp complexes in the BN-PAGE analysis. Details are found under "Materials and methods"

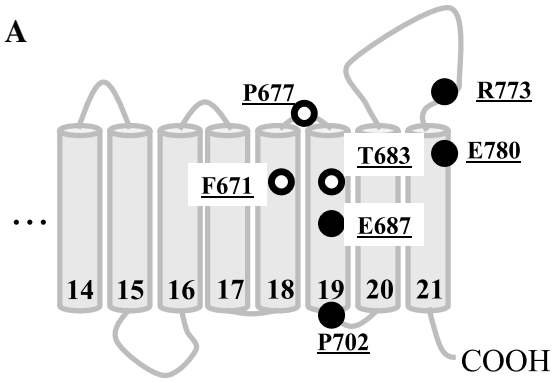

B

```
                          TMS-14
Bp_MrpA      470 HEAPIGMLISPVILGSLVIVFGFFPNILAYTIIEPAMQAVL-PTVLADGELFHVNIYMWHGFNAELFMT
Bh_MrpA      471 HEAPMGMLISPVILGSLVVIFGLFPNLLTYTIIEPAVTAILGADVFGGGE---ANIYLWHGFNPELFMT
Bs_MrpA      467 HEAPVGMLVPPVILVALAVSLFFFPNILSYSLIEPAMNSIY-PTLLDGHEKFHVHISQWHGVTTELLMT
Sm_PhaA/B    476 HEPPRWMRAPLDFLVLACLVVGIIP----AQTIGPFLHTAVLSVLREGTP--DYSLSVWHGWNIPLIMS
Vc_MrpA/B    430 KAIE--QKKSLWLPAMGLAIASFLLPVFALDWIN--QHLVIPAVMAMDPNSVPQAAKLWQGFNIPLALS
                                                                      * *    *
                          TMS-15
Bp_MrpA      538 MGVVAAGIILFLMMKNWAKAAFYMKERDPLN---WFYDSSLSGVITGSQFVTRIQMTGLLRDYFAYMIV
Bh_MrpA      537 IAVVAFGTLIFMNMKKWQQTAFYLRERDPLN---RVYDSSLDWLIKGSQGITRVQMTGMLRDYFAYMCV
Bs_MrpA      535 AGIVVIGTIGYLSLNKWKGIYKLFPSKLTLN---RLYDKLLTMMEKGSYRVTKQYMTGFLRDYLLYIFA
Sm_PhaA/B    539 FVALSGGIGLYFLMRSYLATAVEGPPVFRLLQGQRIFERVLVTLSWKWARWLEQRLGTRRLQPQMRLLV
Vc_MrpA/B    495 GITLVLGGVLYLNYATLVTWLTRLVKPLPKA--EQMFDAVLAYLATLASWQTQMLQQKRSSGYMLLFFA
                     *
                TMS-16                    TMS-17                          TMS-18
Bp_MrpA      604 FMILLLGYTMFRYDAFAIDTTNVTEIAPYIWVITIVFIVATLSIPFIN--KRITAVVVVGVIGFLLALL
Bh_MrpA      603 FMILLFGYTMVRYNAFAIDTVNVSVISPYMWVLTLVFIGSTLAIPFIN--HRITAIIVVGVIGFLLALF
Bs_MrpA      601 GFIILIGGAFAIKGGFSFKTEGMAKIGVYEIILTLVMISATVATVFAR--SRLTAIIALGVVGYTLALF
Sm_PhaA/B    608 FLALAAGASPLLLGNFELPPLVIRGIDPAFALLWAIGIACAIGSAYQAKFHRLASLVLLGGAGLVTCIT
Vc_MrpA/B    562 VLALILIYQPLPLP--ATFSASLFDVHFYEVAIALALIASALLCVLST--SRLLSVLALGMAGFMTTLV
                                                  *                  *  *
                          TMS-19                                    TMS-20
Bp_MrpA      671 FVVFRAPDLALTQLLIETVTVLLLMLAFYHLPELRKE-------EFKPRFN-VLNLIISIGVGFFITAI
Bh_MrpA      670 FVIFRAPDLALTQLLVETVTVVLFMLAFYHLPELRKE-------KFTPRFN-LVNLFISIGVGGLVTLI
Bs_MrpA      668 FVIFRAPDLALTQLVIETISVALFLLCFYHLPKLRLK-------TKTRTFR-MTNFIISLGVGVIVTLL
Sm_PhaA/B    677 FVWLSAPDLAVTQLLVEIVTTVLILLGLRWLPKRIEEPVAAEDISIRVRLRRLRDLLLAIGAGGGMMLI
Vc_MrpA/B    627 FMIYSAPDVAKTLLLVETLMVVFVVLLMRHVPYLSTV-------ARHSVPRRTLNAVIASVIGASVTLI
                 *    *** * *  *  *         *     *                    *     *
                                                                  TMS-21
Bp_MrpA      732 ALSSLALGNEAGIEPISQFFIENSKELAGGYNMVNVILVDFRGLDTMLEVLVLGIAALGVIALIK---
Bh_MrpA      731 ALSSFALGTEAGLGTISEYFIENSKELAGGYNMVNVILVDFRGLDTLLEVLVLGIAALGVIAMIK---
Bs_MrpA      729 GIASSSQRTKD---SIASFFVKHSHDLGGGDNVVNVILVDFRGFDTMFEITVLTIAALGIYSMIK---
Sm_PhaA/B    746 AYTVMTRPLPE---TIASYFLERAYREGGGTNVVNVILVDFRGFDTLGEIAVLCIVALTVFALLLRFRP
Vc_MrpA/B    689 LLNITAHPIDT---TLSDYFAQQSVPGGHGRNIVNVILVDFRAFDTLGEVIVVVMASLVAISLLP---
                                 *         * * *********  **  *  *     *

Bp_MrpA      797 -----LRMTGREDV--
Bh_MrpA      796 -----LRMTGREDV--
Bs_MrpA      791 -----TKVKEEGKSGE
Sm_PhaA/B    816 QSDSLEAPEQQKVQN
Vc_MrpA/B    751 -----KRTEQPQKIHS
```

Fig. 5 Positions of site-directed mutations and deletions in the A-CT domain. **a** The residues in which the mutation reduced antiport activity to 75 % or less than wild type are indicated by *filled circles*. The *open circles* represent residues in which the mutation did not affect the activity relative to wild type. **b** Comparison of sequences in the A-CT domain. The mutated residues are indicated by *bold print*. The *gray highlighted* residues where the TMSs are predicted by all three programs: ConPred II, HMMTOP, and TMHMM. Conserved amino acid residues are indicated with an *asterisk*. See Fig. 1 legend for details

the impressive observations made in this study. The three MrpD mutations, MrpD-D75A, MrpD-R258A and MrpD-F341A, negatively affected antiport activity while the corresponding mutations in MrpA did not lead to any mutant phenotypes. These findings do not necessarily preclude the possibility that NuoL has retained some MrpA-like capacity to translocate sodium that is independent of residues that correspond to the domain shared with MrpD. Several

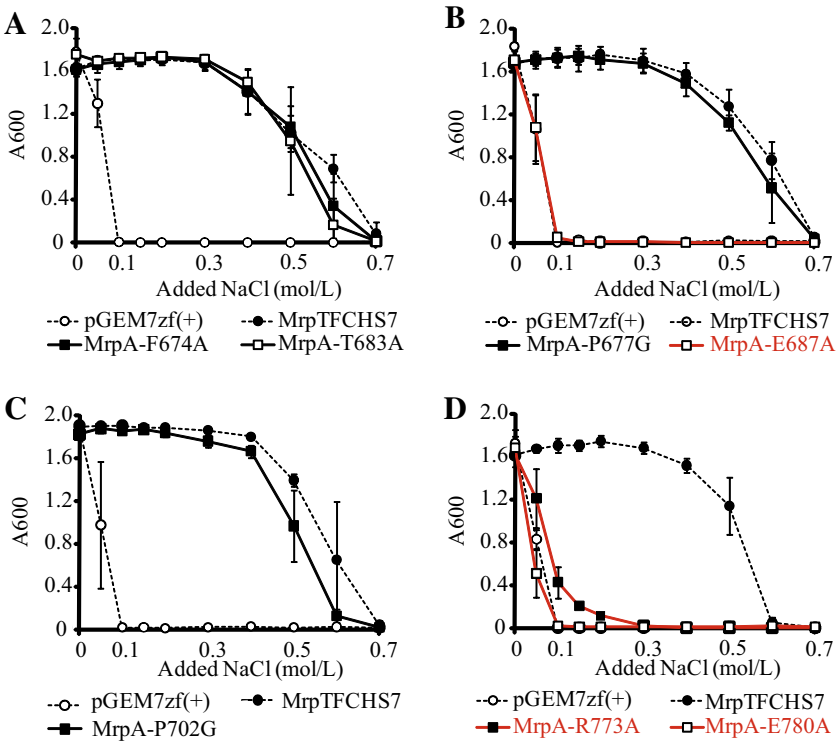

Fig. 6 Effect of mutations in the MrpA A-CT region on capacity of Mrp antiporter to complement the sodium sensitivity of *E. coli* KNabc. See the Fig. 2 legend for details

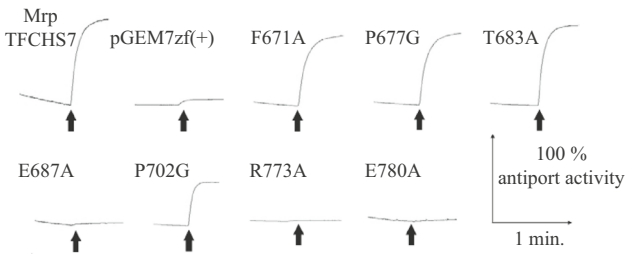

Fig. 7 Florescence-based Na^+/H^+ antiport activity assay of mutations in the MrpA A-CT region. See the Fig. 3 legend for details

studies by others have led to proposals that respiratory complex I may retain a capacity for catalyzing sodium efflux, either by an antiport mechanism when the pump is in a "de-active" form (Roberts and Hirst 2012). Or, perhaps, under some conditions the active complex retains a minor mode of sodium/proton antiport (Batista et al. 2012; Steffen and Steuber 2013). This would be consistent with the finding noted earlier that NuoL from *E. coli* complex I can restore activity to a *mrpA* deletion strain of *B. subtilis* (Moparthi et al. 2011). Recent data on the structure of the mitochondrial complex I should provide a basis for a new model of the "de-active" form (Zickermann et al. 2015).

The crystal structure of *E. coli* complex I reveals three amino acid pairs of NuoL-D82/R268, NuoM-D84/R273 and NuoN-D70/R256 residues that form a salt bridge in each of the three "antiporter-like" subunits. MrpD-D75/R258 may similarly pair to make a salt bridge in the antiporter (Efremov and Sazanov 2011). The MrpD-D75A and MrpD-R258A mutations led not only to diminished antiport activity but also to deficits in formation of Mrp complexes, indicating that those residues participate in Mrp complex stabilization or assembly of the full complex. An earlier study, in which a series of single *mrp* gene deletion mutants was analyzed by BN-PAGE, revealed that MrpD is essential for expression of other Mrp subunits in the cytoplasmic membrane (Morino et al. 2008). These data suggest that MrpD may have an "anchoring" role for the Mrp complex.

The A-CT region of MrpA has no homology to MrpD and NuoLMN subunits. The mutation at MrpA-P677 in the A-CT region resulted in loss of the monomeric full-Mrp complex although it retained the dimeric full-Mrp. The BN-PAGE analysis revealed the monomeric full-Mrp complex as well as the MrpABCD sub-complex and MrpE, MrpF and MrpG subunits in the mutant. This complex formation pattern had been observed the MrpB-P37G and MrpC-Q70A in a previous study (Morino et al. 2010). Thus, the A-CT region, MrpB and MrpC could be important for the interface between the MrpABCD sub-complex and the MrpEFG domain. Mutations at MrpA-E687, -H700 (Morino et al. 2010), -P702, -R773 and -E780 affected antiport activity, which we cannot correlate with a specific lesion (Table 2). However, we note the significant changes in the ratios of Mrp subunit ratios in the group of A-CT mutants, which may ultimately impact on ion translocation (Table 2, expression level).

Two conserved acidic amino acid residues, MrpA-E687 and MrpA-E780, of a putative transmembrane region in the

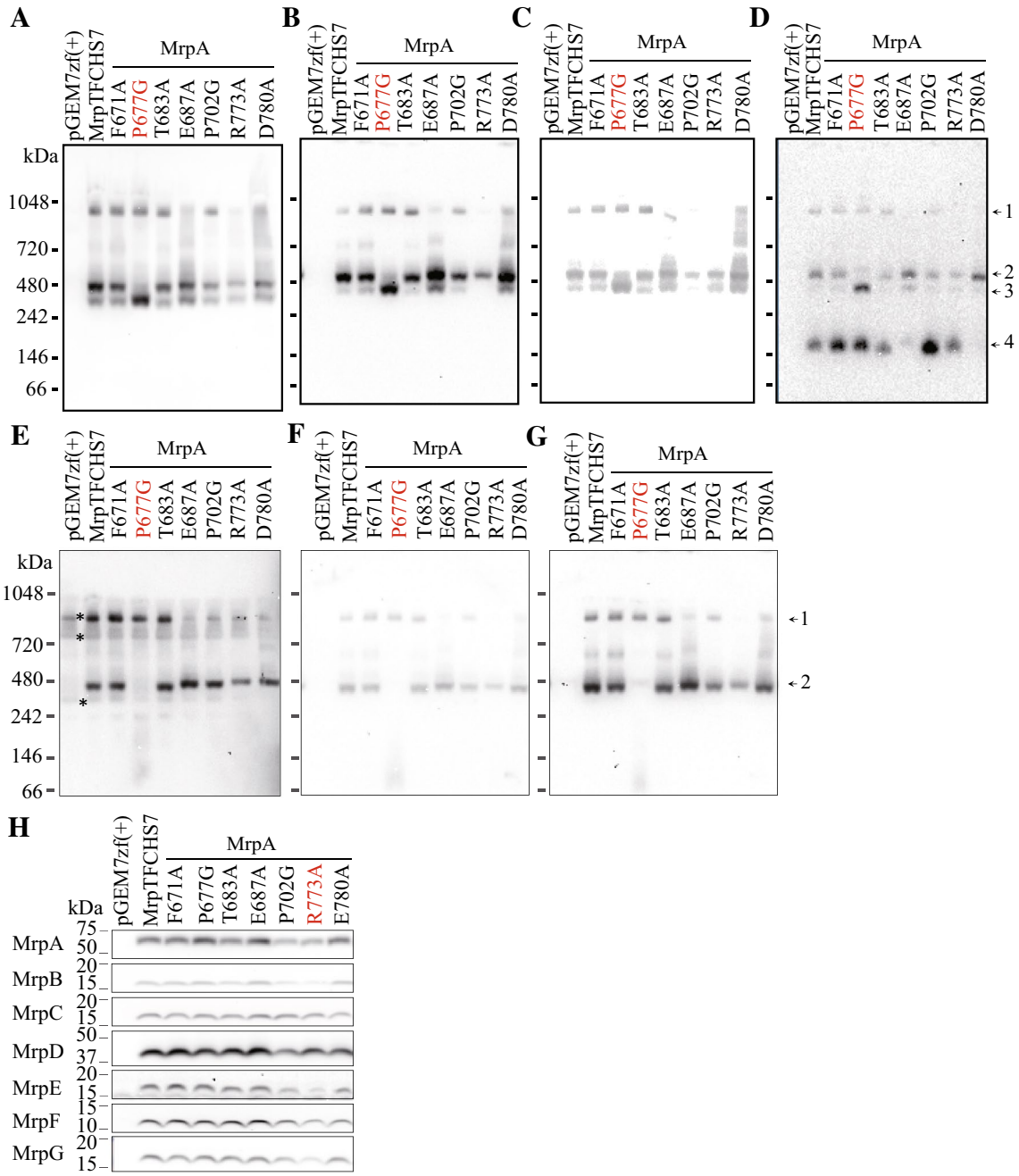

Fig. 8 BN-PAGE and SDS-PAGE analyses and western blot analysis of mutations in the A-CT region. In BN-PAGE, MrpA (**a**), MrpB (**b**), MrpC (**c**), MrpD (**d**), MrpE (**e**), MrpF (**f**) and MrpG (**g**) proteins were detected by western blots using anti-T7 tag antibody, anti-FLAG (DDDDK) tag antibody, anti-*c*-myc tag antibody, anti-penta His tag antibody, anti-MrpE peptide antibody, anti-MrpF peptide antibody or anti-S-tag antibody, respectively. For comparison of expression levels of Mrp subunits in the mutants, thirty micrograms of membrane vesicle proteins was applied to SDS-PAGE gels following western blots (H). The *numbered arrows* on the *right* of the last panel of each BN-PAGE *row* indicate the positions of the MrpABCDEFG dimer (1), the MrpABCDEFG monomer (2), the stable MrpABCD sub-complex (3), and the MrpD dimer (MrpDD) (4), respectively. The *asterisks* in panel **e** indicate nonspecific bands. Details are found under "Materials and methods"

A-CT region are essential for antiport activity. Similar findings have been found in a comparable mutant in *Bacillus subtilis* MrpA, and their importance has been noted (Kajiyama et al. 2009).

The phenotype of MrpA-P702G is very similar phenotype of MrpA-H700 mutants which were reported earlier (Morino et al. 2010). The mutation at MrpA-P702G affected both antiport activity and increased K_M values.

These residues and MrpA-E687 are located in TMS-19 of MrpA, so TMS-19 of MrpA may have a role in cation transport.

MrpA-R773 and MrpA-E780 regions are around the most highly conserved in the A-CT region (Fig. 5b). Since antiport activity was completely lost from both mutants, this conserved region is likely to be a functionally important region. Other fine-tuning factors in the A-CT domain may be clarified by studies of Mrp antiporters with different cation specificities. The Mrp antiporter from *Thermomicrobium roseum* has an aspartate residue at the position corresponding to the *B. pseudofirmus* OF4 MrpA-E687 of the MrpA A-CT region. This Mrp antiporter catalyzes Ca^{2+}/H^{+} antiport (Morino and Ito 2012). It will be of interest to test whether that mutation is responsible or at least required for the change in specificity. This, and perhaps Mrp antiporters with other cation efflux substrates, will be helpful in refining our understanding of the binding sites and the roles of various Mrp antiporter domains.

Acknowledgments This work was supported in part by research grant GM28454 from the National Institute of General Medical Sciences (to T.A.K.), as well as a special research Grant (2010) from Toyo University and JSPS KAKENHI Grant Number 15K07012 (to M.I.).

References

Amarneh B, Vik SB (2010) Transmembrane topology of subunit N of complex I (NADH:ubiquinone oxidoreductase) from *Escherichia coli*. J Bioenerg Biomembr 42:511–516. doi:10.1007/s10863-010-9318-3

Baradaran R, Berrisford JM, Minhas GS, Sazanov LA (2013) Crystal structure of the entire respiratory complex I. Nature 494:443–448. doi:10.1038/nature11871

Batista AP, Marreiros BC, Pereira MM (2012) The role of proton and sodium ions in energy transduction by respiratory complex I. IUBMB Life 64:492–498. doi:10.1002/iub.1050

Brett CL, Donowitz M, Rao R (2005) Evolutionary origins of eukaryotic sodium/proton exchangers. Am J Physiol Cell Physiol 288:C223–C239. doi:10.1152/ajpcell.00360.2004

Efremov RG, Sazanov LA (2011) Structure of the membrane domain of respiratory complex I. Nature 476:414–420. doi:10.1038/nature10330

Hamamoto T, Hashimoto M, Hino M, Kitada M, Seto Y, Kudo T, Horikoshi K (1994) Characterization of a gene responsible for the Na^{+}/H^{+} antiporter system of alkalophilic *Bacillus* species strain C-125. Mol Microbiol 14:939–946

Ito M, Guffanti AA, Wang W, Krulwich TA (2000) Effects of nonpolar mutations in each of the seven *Bacillus subtilis mrp* genes suggest complex interactions among the gene products in support of Na^{+} and alkali but not cholate resistance. J Bacteriol 182:5663–5670

Kaila VR, Wikstrom M, Hummer G (2014) Electrostatics, hydration, and proton transfer dynamics in the membrane domain of respiratory complex I. Proc Natl Acad Sci USA 111:6988–6993. doi:10.1073/pnas.1319156111

Kajiyama Y, Otagiri M, Sekiguchi J, Kudo T, Kosono S (2009) The MrpA, MrpB and MrpD subunits of the Mrp antiporter complex in *Bacillus subtilis* contain membrane-embedded and essential acidic residues. Microbiology 155:2137–2147. doi:10.1099/mic.0.025205-0

Kosono S, Haga K, Tomizawa R, Kajiyama Y, Hatano K, Takeda S, Wakai Y, Hino M, Kudo T (2005) Characterization of a multigene-encoded sodium/hydrogen antiporter (sha) from *Pseudomonas aeruginosa*: its involvement in pathogenesis. J Bacteriol 187:5242–5248. doi:10.1128/JB.187.15.5242-5248.2005

Krulwich TA, Ito M (2013) Prokaryotic alkaliphiles. In: Rosenberg E, DeLong EF, Thompson F, Lory S, Stackebrandt E (eds) The prokaryotes, 4th edn. Springer, New York

Krulwich TA, Sachs G, Padan E (2011) Molecular aspects of bacterial pH sensing and homeostasis. Nat Rev Microbiol 9:330–343. doi:10.1038/nrmicro2549

Lee BL, Sykes BD, Fliegel L (2013) Structural and functional insights into the cardiac Na^{+}/H^{+} exchanger. J Mol Cell Cardiol 61:60–67. doi:10.1016/j.yjmcc.2012.11.019

Lowry OH, Rosebrough NJ, Farr AL, Randall RJ (1951) Protein measurement with the Folin phenol reagent. J Biol Chem 193:265–275

Mathiesen C, Hägerhäll C (2003) The 'antiporter module' of respiratory chain complex I includes the MrpC/NuoK subunit—a revision of the modular evolution scheme. FEBS Lett 549:7–13

Moparthi VK, Hägerhäll C (2011a) The evolution of respiratory chain complex I from a smaller last common ancestor consisting of 11 protein subunits. J Mol Evol 72:484–497. doi:10.1007/s00239-011-9447-2

Moparthi VK, Hägerhäll C (2011b) Recruitment of the antiporter module—a key event in complex I evolution. In: Sazanov LA (ed) A structural perspective on complex I. Springer, Berlin, pp 123–143

Moparthi VK, Kumar B, Mathiesen C, Hägerhäll C (2011) Homologous protein subunits from *Escherichia coli* NADH:quinone oxidoreductase can functionally replace MrpA and MrpD in *Bacillus subtilis*. Biochim Biophys Acta 1807:427–436. doi:10.1016/j.bbabio.2011.01.005

Moparthi VK, Kumar B, AI-Eyani Y, Sperling E, Gorecki E, Drakenberg T, Hägerhäll C (2014) Functional role of the MrpA- and MrpD-homologous protein subunits in enzyme complexes evolutionary related to respiratory chain complex I. Biochim Biophys Acta 1837:178–185. doi:10.1016/j.bbabio.2013.09.012

Morino M, Ito M (2012) Functional expression of the multisubunit type calcium/proton antiporter from Thermomicrobium roseum. FEMS Microbiol Lett 335:26–30. doi:10.1111/j.1574-6968.2012.02634.x

Morino M, Natsui S, Swartz TH, Krulwich TA, Ito M (2008) Single gene deletions of *mrpA* to *mrpG* and *mrpE* point mutations affect activity of the Mrp Na^{+}/H^{+} antiporter of alkaliphilic *Bacillus* and formation of hetero-oligomeric Mrp complexes. J Bacteriol 190:4162–4172. doi:10.1128/JB.00294-08

Morino M, Natsui S, Ono T, Swartz TH, Krulwich TA, Ito M (2010) Single site mutations in the hetero-oligomeric Mrp antiporter from alkaliphilic *Bacillus pseudofirmus* OF4 that affect Na^{+}/H^{+} antiport activity, sodium exclusion, individual Mrp protein levels, or Mrp complex formation. J Biol Chem 285:30942–30950. doi:10.1074/jbc.M110.118661

Nakamaru-Ogiso E, Kao MC, Chen H, Sinha SC, Yagi T, Ohnishi T (2010) The membrane subunit NuoL(ND5) is involved in the indirect proton pumping mechanism of *Escherichia coli* complex I. J Biol Chem 285:39070–39078. doi:10.1074/jbc.M110.157826

Nozaki K, Kuroda T, Mizushima T, Tsuchiya T (1998) A new Na^{+}/H^{+} antiporter, NhaD, of *Vibrio parahaemolyticus*. Biochim Biophys Acta 1369:213–220

Orlowski J, Grinstein S (2007) Emerging roles of alkali cation/proton exchangers in organellar homeostasis. Curr Opin Cell Biol 19:483–492. doi:10.1016/j.ceb.2007.06.001

Padan E, Venturi M, Gerchman Y, Dover N (2001) Na^+/H^+ antiporters. Biochim Biophys Acta 1505:144–157

Padan E, Bibi E, Ito M, Krulwich TA (2005) Alkaline pH homeostasis in bacteria: new insights. Biochim Biophys Acta 1717:67–88. doi:10.1016/j.bbamem.2005.09.010

Ren Q, Chen K, Paulsen IT (2007) TransportDB: a comprehensive database resource for cytoplasmic membrane transport systems and outer membrane channels. Nucleic Acids Res 35:D274–D279. doi:10.1093/nar/gkl925

Rimon A, Tzubery T, Padan E (2007) Monomers of the NhaA Na^+/H^+ antiporter of *Escherichia coli* are fully functional yet dimers are beneficial under extreme stress conditions at alkaline pH in the presence of Na^+ or Li^+. J Biol Chem 282:26810–26821

Roberts PG, Hirst J (2012) The deactive form of respiratory complex I from mammalian mitochondria is a Na^+/H^+ antiporter. J Biol Chem 287:34743–34751. doi:10.1074/jbc.M112.384560

Saier MH Jr, Yen MR, Noto K, Tamang DG, Elkan C (2009) The transporter classification database: recent advances. Nucleic Acids Res 37:D274–D278. doi:10.1093/nar/gkn862

Sato M, Sinha PK, Torres-Bacete J, Matsuno-Yagi A, Yagi T (2013) Energy transducing roles of antiporter-like subunits in *Escherichia coli* NDH-1 with main focus on subunit NuoN (ND2). J Biol Chem 288:24705–24716. doi:10.1074/jbc.M113.482968

Schuldiner S (2014) Competition as a way of life for H^+-coupled antiporters. J Mol Biol 426:2539–2546. doi:10.1016/j.jmb.2014.05.020

Steffen W, Steuber J (2013) Cation transport by the respiratory NADH:quinone oxidoreductase (complex I): facts and hypotheses. Biochem Soc Trans 41:1280–1287. doi:10.1042/BST20130024

Steimle S, Willistein M, Hegger P, Janoschke M, Erhardt H, Friedrich T (2012) Asp563 of the horizontal helix of subunit NuoL is involved in proton translocation by the respiratory complex I. FEBS Lett 586:699–704. doi:10.1016/j.febslet.2012.01.056

Sturr MG, Guffanti AA, Krulwich TA (1994) Growth and bioenergetics of alkaliphilic *Bacillus firmus* OF4 in continuous culture at high pH. J Bacteriol 176:3111–3116

Swartz TH, Ikewada S, Ishikawa O, Ito M, Krulwich TA (2005) The Mrp system: a giant among monovalent cation/proton antiporters? Extremophiles 9:345–354. doi:10.1007/s00792-005-0451-6

Swartz TH, Ito M, Ohira T, Natsui S, Hicks DB, Krulwich TA (2007) Catalytic properties of *Staphylococcus aureus* and *Bacillus* members of the secondary cation/proton antiporter-3 (Mrp) family are revealed by an optimized assay in an *Escherichia coli* host. J Bacteriol 189:3081–3090. doi:10.1128/JB.00021-07

Torres-Bacete J, Nakamaru-Ogiso E, Matsuno-Yagi A, Yagi T (2007) Characterization of the NuoM (ND4) subunit in *Escherichia coli* NDH-1: conserved charged residues essential for energy-coupled activities. J Biol Chem 282:36914–36922. doi:10.1074/jbc.M707855200

Virzintiene E, Moparthi VK, Al-Eryani Y, Shumbe L, Gorecki K, Hägerhäll C (2013) Structure and function of the C-terminal domain of MrpA in the *Bacillus subtilis* Mrp-antiporter complex–the evolutionary progenitor of the long horizontal helix in complex I. FEBS Lett 587:3341–3347. doi:10.1016/j.febslet.2013.08.027

Zickermann V, Wirth C, Nasiri H, Siegmund K, Schwalbe H, Hunte C, Brandt U (2015) Structural biology. Mechanistic insight from the crystal structure of mitochondrial complex I. Science 347:44–49. doi:10.1126/science.1259859